Ad Hoc Networks 118 (2021) 102517

Contents lists available at ScienceDirect

Ad Hoc Networks

journal homepage: www.elsevier.com/locate/adhoc

Energy-efficient and solar powered mission planning of UAV swarms to reduce the coverage gap in rural areas: The 3D case

Jaime Galán-Jiménez *, Enrique Moguel, José García-Alonso, Javier Berrocal

University of Extremadura, Cáceres, Spain

ARTICLE INFO

Keywords:
UAV
Energy efficiency
Rural areas
Coverage gap
GA

ABSTRACT

Although the percentage of people living outside a broadband network has more than halved in recent years, around 10% of the global population does not have access to the Internet. This lack of coverage is particularly concentrated in rural and low-income areas, in which the lack of a cost-effective electricity supply is the main barrier to expanding network coverage. To tackle this problem, this work proposes a theoretical model based on a self-sustainable 5G network architecture in which the mission planning of a swarm of Unmanned Aerial Vehicles (UAVs) is efficiently scheduled to provide cellular coverage over the territory and to reduce the required energy consumption. A Mixed Integer Linear Programming is provided to formalize the problem of minimizing the energy consumption required by the swarm of UAVs that are able to provide coverage by operating at different altitudes. In order to practically solve the problem, a Genetic Algorithm is defined and evaluated over a realistic scenario. Results indicate that a higher granularity in the number of altitudes at which UAVs can provide coverage increases the percentage of territory that is covered, while a small penalty on the energy consumption must be paid compared to the case in which an unique altitude over the ground is considered.

1. Introduction

Mobile networks are the most common method to access the Internet for the majority of the world's population. In fact, mobile technology is the easiest (and in many cases the only) way to allow low-income populations and rural residents to be connected [1]. Although the mobile industry connects over 3.5 billion people around the world (47% of the global population), around 10% of the population is still not covered by mobile broadband, i.e., a 3G connection or higher. This percentage, also known as *coverage gap*, is mostly concentrated in rural and remote areas (e.g., Sub-Saharan Africa or South Asia), where up to 40% of the population cannot have access to 3G connectivity [2]. If no actions are performed to reduce the coverage gap in the near future, the risk of reinforcing existing inequalities among people living in those areas will still be present.

The main reason associated to the coverage gap is the prohibitive cost of mobile broadband deployment in rural and low-income areas. The cost of construction and management of the required network infrastructure in a rural area is, on average, double compared to the case of an urban deployment. Moreover, the revenue obtained in these locations is normally of the order of 10 times lower than the one retrieved in a city. In particular, the cost of a mobile network infrastructure, including both operator's capital (CapEx) and operational expenditure (OpEx), can be divided into three areas: (i) the mobile Base Station (BS) deployment; (ii) the back-haul technology connecting the user to the core network; and (iii) the energy that is required to make these elements functional, both supply and storage.

In the recent years, the networking research community has exploited the emergence of Unmanned Aerial Vehicles (UAVs) to propose a new concept of cellular network, in which UAVs carry a BS to provide cellular coverage over a portion of territory [3,4]. Solutions such as the Altaeros SuperTower [5] and Loon [6] aim at reducing the operational costs of providing cellular coverage to disperse populations. UAV-based cellular networks provide a better spatial and temporal flexibility compared to traditional-fixed cellular networks, since specific areas and time spans can be selected for coverage provisioning. Nevertheless, a major drawback arises in the main component of the architecture: the UAVs battery depletion derived from their coverage operation [3]. UAVs are generally equipped with limited batteries that must be frequently recharged [7,8]. In most cases, recharging operations normally require the connection of ground sites to the electricity grid, which would increase the associated cost.

To overcome this challenge, renewable energy solutions, particularly the solar-powered ones, are an interesting common solution for many rural deployments. They can provide energy to ground sites

* Corresponding author.
E-mail addresses: jaime@unex.es (J. Galán-Jiménez), enrique@unex.es (E. Moguel), jgaralo@unex.es (J. García-Alonso), jberolm@unex.es (J. Berrocal).

https://doi.org/10.1016/j.adhoc.2021.102517
Received 29 September 2020; Received in revised form 25 March 2021; Accepted 31 March 2021
Available online 10 April 2021

designed to function off-grid or to serve specific remote rural communities [8]. Therefore, exploiting the optimal installation of a set of Solar Panels (SPs) in specific locations can serve as the basis for the proposal of sustainable UAV-based cellular networks able to provide coverage in rural and low-income areas. In [8], the authors propose an energy-efficient UAV mission planning scheme to solve the coverage problem in rural areas throughout time. In particular, the objective of such work is to maximize the energy stored by the set of UAVs and the one stored in the batteries of the ground sites, while ensuring the coverage and energy constraints. However, the impact of the UAVs altitude on the energy consumption is not considered, i.e., the multi-period mission planning is formulated and solved considering a 2D case scenario. As reported in the literature, ascending/descending actions must be carefully considered when proposing an energy-efficient mission planning solution for UAV swarms [9,10]. These actions clearly impact UAVs battery levels and must be taken into account to prevent from potential battery depletion before the UAV with low battery moves to a ground site in order to recharge it.

In this work we define and solve the 3D problem, in which UAVs are able to fly and provide coverage at different altitudes. The motivation is derived by the fact that if an UAV is hovering at a higher altitude, the coverage range is bigger compared to the case where the UAV altitude is lower. Nevertheless, the higher the altitude of the UAV, the higher energy consumption required to provide coverage. This trade-off must be carefully evaluated and it is a fundamental aspect in energy-efficient UAV-based solutions. In this context, several questions emerge, such as: Is it possible to define a model to cover a set of areas by means of a swarm of UAVs that can be placed at different altitudes and manage their energy consumption in an efficient manner? How to leverage the trade-off between the altitudes at which UAVs should be placed and the energy consumption required for a successful and energy-efficient mission planning? Is it possible to define a strategy to solve this problem in tractable time? These issues are not targeted by [8], while in this paper they are faced and analyzed to a large extent.

In particular, a theoretical model is provided to schedule energy-efficient missions by exploiting UAV-based 5G networks. The proposed model is composed of an energy measurement tool which relies on different specifications for UAV actions, coverage, and path loss. In addition, the formalization of the 3D Energy-Efficient UAVs Mission Planning (3DEE-UMP) problem is provided. Eventually, an heuristic based on Genetic Algorithms (GAs) is defined to solve the problem in a reasonable amount of time. The obtained results reveal that the possibility of considering a higher number of altitudes improves the percentage of the target scenario that is covered by the set of UAVs, while a small penalty on the energy consumption must be paid w.r.t. the case in which only one altitude over the ground is considered.

The remainder of the paper is organized as follows. Section 2 reviews the related work. In Section 3, the proposed UAV-based 5G network architecture is defined. Section 4 presents the problem formulation that aims at solving the problem at hand. The GA-based heuristic is described in Section 5. Section 6 reports the performance evaluation of the proposed solution. Finally, Section 7 concludes our work and introduces future research lines.

2. Related work

In the last few years, different proposals [4,11] have been defined for optimally placing UAVs in order to improve the network coverage in different areas. Some works, such as [12,13], focus on improving the performance and the throughput of wireless networks by means of UAVs. Concretely, in [12], the authors focus on evaluating the multi-UAVs' trajectory and power control in order to maximize the minimum throughput over all ground users. To that end, they propose a convex iterative optimization algorithm. In [8], some of the authors of this paper proposed a technique to provide wireless coverage in rural and low-income areas by means of UAVs powered by SPs and batteries. In this approach a brand-new GA was proposed for maximizing the energy stored (both at the ground stations for future needs and at the UAVs for performing the coverage missions) and the territory covered by efficiently planning different missions. Nevertheless, only a 2D scenario was considered. These works do not consider the altitude of the UAVs to improve the throughput nor the energy consumed by the UAVs.

Recently, different 3D placement methods have been proposed [14,15]. For instance, in [14] the authors decouple the UAVs deployment problem in the vertical and horizontal dimensions considering also the transmit power in order to increase the number of covered users using the minimum required transmit power. Similarly, in [15], the authors focus on assuring a minimum quality of service (per-user coverage probability and per-user rate) by optimizing the total power consumed (dependent on the number of UAV-BS and their transmit power) by the system. This optimization of the total power consumed allows the authors to reduce the operational cost induced by the energy consumption. However, as detailed in the previous section, these proposals do not consider the cost of deploying a power grid in rural environments. In addition, different UAVs can also be coordinated to increase the covered area and to reduce resource consumption.

There are also other proposals, such as [9], designing the trajectory and the resource allocation for UAVs powered by SPs. In [9], the authors apply mixed-integer non-convex and monotonic optimization techniques in order to identify the best trade-off and balance between the solar energy harvested by the UAVs (with SPs) and the power needed to achieve and maintain the QoS required by the users. These techniques are applied over multi-carrier UAVs, so that the best subcarrier is also selected. In this work, we focus on battery powered UAVs that can use external SPs to recharge the batteries, so that the UAVs do not have to be placed in a specific location in order to harvest the required solar energy. In addition, we also focus on how a swarm of UAVs can be coordinated and placed at different altitudes in order to improve the connectivity of the coverage area.

In this sense, in [16,17], the authors focus on how to improve network coverage by using a UAV swarm context. To that end, they defined different recommendation for designing an ultra-reliable communication system modifying the software protocol stack and the RF hardware [16]. In addition, different optimization solutions have been defined to minimize the number of UAVs required to provide coverage to a given area [18], the charging time, the traveling time and the number of subareas covered [17]. For instance, in [19], and iterative algorithm is proposed to decouple the joint optimization of the bandwidth-and-power allocation, horizontal placement and vertical placement in order to improve the max–min rate for multi-UAV. Nevertheless, these works do not consider that the UAV swarm can be placed at different altitudes in order to maintain the required QoS levels and also to reduce the energy consumption.

Finally, different works also analyze the placement and the transmit power of UAVs in order to improve the coverage in different scenarios. In [20], the authors consider the problem on optimal 3D placement of UAV-BS in order to maximize the life-time of the mobile ad hoc network. To that end, they evaluate the most efficient circuit power depending on the mobile user's density. The authors identify that, in dense scattering environments, the slope is large, and the optimal hovering altitude is higher than in sparse scattering environments. In addition, the user's density directly affects the coverage radius. Similar results are obtained by [21], in which different environment (i.e., sub-urban, urban dense urban and high-rise urban) for temporary events are evaluated for the placement of UAV-BS in order to accommodate the aerial channel model. These studies also reveal that the height of the UAV-BS and the propagation environment affect the network performance. Other works, such as [22], focus on the UAV-content delivery for rural environments and irregular terrains, proposing the broadcasting of content with UAVs at different altitudes in order to improve the efficiency in this environments. Therefore, the best selection of the transmit power highly depends on the targeted scenario [21]. In this paper, we focus on planning UAV swarms missions in rural environments, but also reducing the energy consumption.

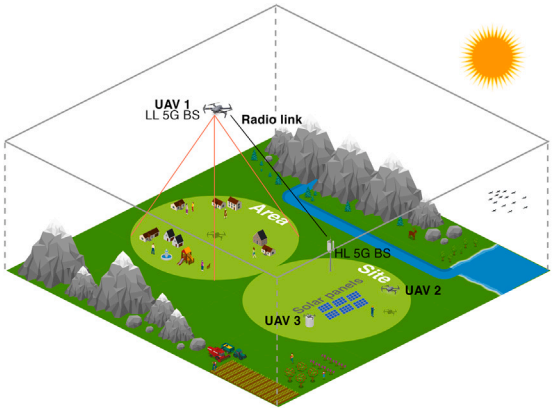

Fig. 1. Proposed self-sustainable UAV-based 5G architecture providing coverage in a remote area.

3. UAV-based 5G network model

In this section, the description of the theoretical model for the scheduling of energy-efficient missions of UAVs to provide coverage in rural areas is provided. At first, the considered UAV-based 5G network architecture is described. It is based on our previous work [8], where the target location over which to provide 5G connectivity is divided into a set of places. Two types of places are considered, namely *areas* and *sites*. An *area* is a portion of territory in which coverage must be always ensured (i.e., 24/7) by, at most, one UAV. A ground *site* is a place where a set of SPs and batteries are installed (charging stations). In our approach, a site is co-located with an area, and it is normally placed at the center of the area.

Fig. 1 shows a scenario in which the proposed UAV-based 5G network architecture is represented. UAVs are equipped with a 5G BS, which is mounted on top of it in order to provide 5G coverage over an area. Low Level (LL) BS functionalities are carried by the proper UAV, while the High Level (HL) ones are installed at a site. A radio link between the UAV and the site is able to connect both HL and LL functionalities. Clearly, a constraint in the maximum distance between the area and the corresponding site must be imposed. Otherwise, the degradation of the signal strength could prevent the connection. Inter-UAV communication is assumed to be enabled by a third radio system. Moreover, the interference between UAVs that are serving adjacent areas is minimized with the selection of the size of the areas, as well as with the distance between the center of two adjacent areas. Regarding the radio resources that are assigned to the areas, it is assumed that (i) the throughput served to the users is equally provided along the area; (ii) there is a guarantee of Line of Sight (LoS) w.r.t. the user due to the fact that the altitude of the UAV does not impact the link between LL and HL functionalities. The proposed model is intended to be applied over open rural areas where the existing infrastructure (small individual houses) does not affect the network performance in terms of interference. Moreover, pleasant conditions are also assumed, so that UAVs can operate properly.

The proposed 5G UAV-based architecture is self-sustainable, in the sense that each UAV is equipped with a battery and is able to move toward a ground site in order to be recharged if necessary. Clearly, sites must include equipment able to (i) retrieve energy from the sun (SPs) and (ii) recharge UAVs batteries.

3.1. UAVs actions model and mission planning

In order to provide continuous coverage over the target scenario, an UAV is able to perform a set of actions, ranging from ascending from a ground site to a specific altitude, moving between areas at a given height, covering a specific area or staying at a site. Furthermore, a mission of an UAV requires the scheduling of a set of actions. We divide the time sequence (e.g., one day) into Time Slots (TS), and the duration of each action involves one TS. The duration of a TS is considered as a parameter, which gives us the opportunity to evaluate our solution with different types of UAVs and energy consumption models. It is assumed that for each action, the communication between the UAV and the corresponding site is available. Differently from our previous work [8], in this work we consider that UAVs are able to fly and provide coverage at different altitudes. The motivation is derived by the fact that if an UAV is hovering at a higher altitude, the coverage range is bigger compared to the case where the UAV altitude is lower [4]. However, the higher the altitude of the UAV, the higher energy consumption required to provide coverage [9]. This trade-off must be carefully evaluated and it is a fundamental aspect in energy-efficient UAV-based solutions.

Table 1
UAV actions model in a generic scenario.

Action (at TS t)	Start place	Destination place	Altitude
STAY	s_i	s_i	h_0
REC	s_i	s_i	h_0
COV	z_i	z_i	$h_k, k \in [1, \lvert\mathcal{H}\rvert]$
MOV	z_i	z_j	$h_k, k \in [1, \lvert\mathcal{H}\rvert]$
ASC	$p_i(s_i \vee z_i)$	$z_i \vee z_j$	$h_k, k \in [1, \lvert\mathcal{H}\rvert]$
DESC	z_i	$p_i(s_i \vee z_i) \vee p_j(s_j \vee z_j)$	$h_k, k \in [0, \lvert\mathcal{H}\rvert - 1]$

In the proposed UAVs actions model, the following actions are considered: (i) STAY: The UAV is staying at a ground site and not consuming energy at all; (ii) REC: The UAV batteries are recharged at a ground site; (iii) COV: The UAV is providing coverage over an area; (iv) MOV: The UAV is moving from an area to an adjacent one without modifying its altitude; (v) ASC: The UAV ascends from a site to an area or from an area to another one with an upper altitude level; and (vi) DESC: The UAV descends from an area to a site or from an area to another one with a lower altitude level.

Table 1 reports the set of actions of the proposed UAVs actions model. Each row defines a specific action at a particular TS. Each action can be represented as an arc (colored arrow in Fig. 2) where the tail is the starting place of the action (s_i if it is a site or z_i if it is an area) and the head is the destination place. In case an action can be started or finished regardless the type of place, i.e., it does not matter if it is a site or an area, term p_i (for place) has been used. The last column of Table 1 indicates the altitude at which such action is performed. For the sake of simplicity, it refers to the altitude at which the UAV is placed over the action destination place. Clearly, both STAY and REC actions can be only performed at ground level (h_0).

An example of possible actions performed by the set of UAVs in a scenario composed of two places, $\mathcal{P} = \{p_i, p_j\}$, with two sites, $\mathcal{S} = \{s_i, s_j\}$, and two areas, $\mathcal{Z} = \{z_i, z_j\}$, where UAVs can be placed at two possible altitudes, $\mathcal{H} = \{h_0, h_1\}$, ($h_0$, ground level, and h_1 [m]) is reported in Fig. 2(a). Considering this setting, 16 possible actions can be executed by each UAV. In case an additional altitude is considered in the same scenario, $\mathcal{H} = \{h_0, h_1, h_2\}$, with h_0 as ground level and $d(h_0, h_1) = d(h_1, h_2)$, i.e., the same distance holds between h_0 and h_1, as well as between h_1 and h_2, all the possible actions that can be executed in the scenario are depicted in Fig. 2(b). Thus, the potential number of actions in this 3-altitude model increases up to 28. It is therefore clear that the increase in the number of places and in the number of altitudes for the UAVs certainly impacts the problem complexity. Differently from the 2-altitude model (Fig. 2(a)), in this model there are two altitudes at which an UAV is able to cover, h_1 and h_2. If the UAV is covering at the highest altitude, h_2, it provides coverage to a bigger area compared to the case in which the same UAV is covering at h_1. As a drawback, the energy consumed by the UAV placed at a higher altitude is also larger, leading to the schedule of early recharging actions. Fig. 3 depicts the trade-off described above.

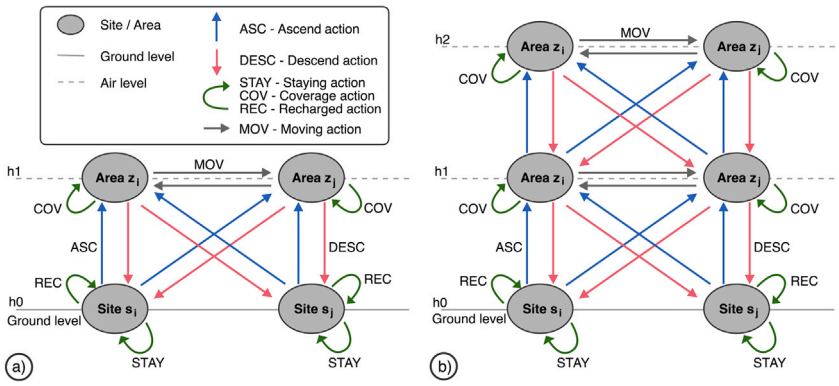

Fig. 2. Set of UAV actions between two sites and two areas considering (a) two altitudes, $\mathcal{H} = \{h_0, h_1\}$, and (b) three altitudes, $\mathcal{H} = \{h_0, h_1, h_2\}$.

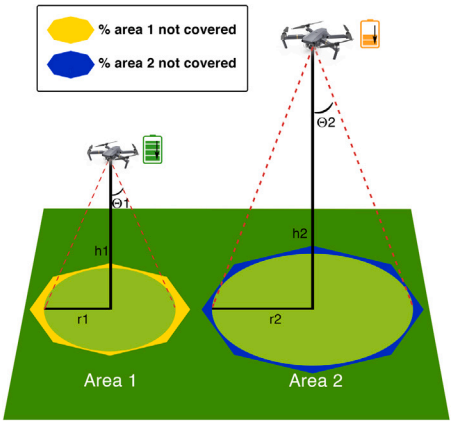

Fig. 3. Example of coverage range achieved by an UAV as a function of the altitude.

3.2. UAVs coverage model

UAVs are assumed to have a conical antenna propagation pattern as in Fig. 3, with an angle of θ. Their projection on the ground is assumed to be a circular area, whose radius, r, depends on its altitude, h_k, according to Eq. (1):

$$r = h_k \cdot \tan(\theta) \tag{1}$$

where θ represents the conical angle of the radiation pattern for the UAV. Since we consider an area as a polygon (see Fig. 3), the circular coverage of a particular UAV that is placed onto the center of the area at altitude h_k could lead to have small portions of the target area that are not actually covered (normally at the edge of the area). In this way, we divide the set of areas in the scenario according to a Voronoi Tesselation in such a way that the aggregated portion of each area that is not covered is minimal. The proposed solution ensures full coverage 24/7 to each of the areas in the scenario by scheduling the movement of the UAVs through the action set defined in Section 3.1. In case an UAV is covering an area and its battery is below a threshold, another UAV is ready to ascend and cover the target area during the following TSs.

3.3. UAVs path loss model

In order to select the optimal altitude, h^{OPT}, we now define the path loss model that has been considered in our solution. Based on the one defined in [14,23], the probabilistic mean path loss between an UAV that is placed at altitude h_k over a location $z = (x, y)$ is defined by Eq. (2):

$$\chi(h_k, r_i) = \frac{A}{1 + d \cdot \exp(-e \cdot (\frac{180}{\pi}) \tan^{-1}(\frac{h_k}{r_i}) - d)} + 10 \log(h_k^2 + r_i^2) + B \tag{2}$$

where $A = \eta_{\text{LoS}} - \eta_{\text{NLoS}}$, and $B = 20 \cdot \log(\frac{4\pi f_c}{c}) + \eta_{\text{NLoS}}$. The average additional losses for Line of Sight (LoS) and No Line of Sight (NLoS) conditions are represented by η_{LoS} and η_{NLoS}, respectively. Moreover, d and e are the S-curve parameters that depend on the environment [23], f_c is the carrier frequency and r_i is the distance between the center of the UAV and user i, as in Eq. (3):

$$r_i = \sqrt{(x_i - x)^2 + (y_i - y)^2} \tag{3}$$

Thus, user i is covered by the UAV placed at altitude h_k if its probabilistic mean Signal-to-Noise Ratio (SNR) is above a predefined threshold $\gamma(h_k, r_i)$, according to Eq. (4):

$$\gamma(h_k, r_i) = P_t - \chi(h_k, r_i) - P_n \tag{4}$$

where P_t and P_n are the transmit power of the UAV and the noise power at the ground site, respectively.

In [23], the authors state that the optimal elevation angle (θ in Eq. (1)) depends on the specific environment where the UAV is deployed (suburban — 20.34°, urban — 42.44°, dense urban — 54.62°, high-rise urban — 75.52°). Knowing the optimal value of θ for a given environment, the maximum coverage radius r can be obtained by solving Eq. (2). Thus, the optimal altitude h_k at which the UAV is able to cover a specific area with minimum loss can be calculated by solving Eq. (1). Although the main goal of this work is to optimally calculate the UAVs mission planning in terms of energy efficiency, the set of altitudes at which the UAVs swarm can operate must be previously assessed and passed to the model as input. We remark that the path loss model defined above is considered for the type of scenario for which the proposed solution is conceived, i.e., open rural areas in which there is a lack of interference due to the existing infrastructure and neighboring UAVs.

3.4. UAVs energy consumption model

Regarding the UAVs energy consumption, all the actions defined in Section 3.1 and reported in Table 1 consume an amount of energy except the STAY action, in which the UAV is placed on a ground site and does not consume any energy during a time period δ_t, i.e., $E^{\text{STAY}}(\delta_t) = 0$ [Wh]. On the contrary, the recharging action (REC) to feed UAVs batteries on a site requires an amount of energy $E^{\text{REC}}(\delta_t)$ [Wh], which is provided by the batteries connected to the SPs that acquired the energy. The energy consumption model for STAY and REC actions is adopted from our previous work [8], where an energy-efficient mission planning is provided for the 2D case.

Concerning the coverage action (COV), where an UAV is hovering over an area at a particular altitude, we use the empirical energy consumption model defined in [24], which is based on real measurements with electrical motors and data from UAV vendors. More formally, the energy consumption of an UAV that is hovering at altitude h_k during a time period δ_t is defined by Eq. (5):

$$E^{\text{COV}}(\delta_t) = (\beta + \alpha \cdot h_k) \cdot \delta_t + P_s^{h_k} \tag{5}$$

where β is the least power required to minimally hover over the ground, and α is a motor speed multiplier which is related to the power required to ascend to altitude h_k. Both parameters, α and β depend on the UAV weight and the features of its motor. $P_s^{h_k}$ represents the power consumption required to lift the UAV to height h_k with speed s. As previously introduced, term δ_t represents the duration of the UAV coverage action, which clearly impacts the energy consumed by the UAV. Eq. (5) relates the power consumption needed by the UAV to lift up using a specific speed and, after that, hover over the target area. However, a new component that also impacts the energy consumption must be considered when the UAV is performing a COV action: the functionality of the BS that is mounted on top of it serving the users located in the area. Adopting the model from [25], this amount of energy is given by Eq. (6):

$$E^{\text{BS}}(\delta_t) = P^{\text{BS}} \cdot \delta_t \tag{6}$$

where P^{BS} represents the power consumption when the BS radio is active to serve the set of users in the area. This functionality is only in working state while the UAV is covering an area. For the rest of the actions, $P^{\text{BS}} = 0$. Therefore, by combining Eqs. (5) and (6), the UAV energy consumption while it is performing a COV action is defined by Eq. (7):

$$E^{\text{COV}}(\delta_t) = (\beta + \alpha \cdot h_k) \cdot \delta_t + P_s^{h_k} + P^{\text{BS}} \cdot \delta_t \tag{7}$$

Regarding the subset of moving actions, in which the UAVs can ascend or descend toward an area/site (ASC/DESC actions), or move at same altitude toward another area (MOV action), we adopt the energy consumption model defined in [9]. The vertical energy consumption, E_v, of an UAV while it ascends or descends during a time interval δ_t is given by Eq. (8):

$$E_v(\delta_t) = m \cdot g \cdot V_v(\delta_t) \cdot \delta_t \tag{8}$$

where m is the mass of the UAV, g is the gravitational acceleration, and $V_v(\delta_t)$ is the UAV vertical speed, i.e., the velocity of the UAV acquired to ascend/descend during time period δ_t. In particular, $V_v(\delta_t)$ is represented by Eq. (9):

$$V_v(\delta_t) = \begin{cases} \dfrac{h_k}{\delta_t} & \text{if the UAV ascends} \\ -\dfrac{h_k}{\delta_t} & \text{if the UAV descends} \end{cases} \tag{9}$$

where h_k is the vertical distance of the UAV flight. If the UAV is ascending (ASC action), the value of $V_v(\delta_t)$ is positive. On the contrary, a negative number is obtained when the UAV is descending (DESC action), due to the fact that the flight has the same direction of the gravitational acceleration force. Thus, the vertical energy consumption is associated to actions in which either (i) the UAV moves to an upper altitude level; or (ii) the UAV descends to a lower level.

Apart from the vertical energy consumption, E_v, an horizontal energy consumption component must be added to the energy consumed by the UAVs while they are flying, i.e., when MOV, ASC and DESC actions are performed. This horizontal energy consumption, E_h, during time period δ_t is defined by Eq. (10):

$$E_h(\delta_t) = \frac{(m \cdot g)^2}{\sqrt{2} \cdot \rho \cdot a} \cdot \frac{1}{\sqrt{V_h(\delta_t)^2 + \sqrt{V_h(\delta_t)^4 + 4 \cdot E_{\text{hov}}(\delta_t)^4}}} \cdot \delta(t) \tag{10}$$

Table 2
UAVs energy consumption model.

Action (during δ_t)	Energy consumption	Reference/s
STAY	0 [Wh]	[8]
REC	0 [Wh]. The UAV is actually receiving E^{REC} energy	[8]
COV	$E^{\text{COV}}(\delta_t) = (\beta + \alpha \cdot h_k) \cdot \delta_t + P_s^{h_k} + P^{\text{BS}} \cdot \delta_t$	[24,25]
MOV	$E^{\text{MOV}}(\delta_t) = E_h(\delta_t) + E_r(\delta_t)$	[9]
ASC	$E^{\text{ASC}}(\delta_t) = E_h(\delta_t) + E_v(\delta_t) + E_r(\delta_t)$	[9]
DESC	$E^{\text{DESC}}(\delta_t) = E_h(\delta_t) + E_v(\delta_t) + E_r(\delta_t)$	[9]

where ρ is the density of the air, a is the area of the rotor disks of the UAV, $V_h(\delta_t)$ is the UAV horizontal speed defined by Eq. (11), and E_{hov} is the energy consumed by the UAV when it is hovering over the area:

$$V_h(\delta_t) = \frac{d(p_1, p_2)}{\delta_t} \tag{11}$$

$$E_{\text{hov}}(\delta_t) = \sqrt{\frac{m \cdot g}{2 \cdot \rho \cdot a}} \tag{12}$$

In Eq. (11), $d(p_1, p_2)$ represents the distance between places p_1 and p_2. Specifically, the distance is computed considering the center of both places. By looking at Eq. (10), and initially at the numerator, it is clear to see that the higher the UAV mass is, m, the higher energy consumption associated to its horizontal flight. On the other hand, an increase in the rotor disks area, a, can better exploit the lift provided by the air flow, which results in a decrease in the energy consumption. The same situation arises for V_h, in whose case the higher horizontal speed achieved by the UAV, the better energy efficiency thanks to the help of the air flow, which increases the lift of the UAV. E_{hov} is also inversely proportional to E_h, and the duration of the flight δ_t again impacts the UAV energy consumption.

In addition, it is also necessary to take into account the resistance of the UAV blades against the air, which is expressed by Eq. (13):

$$E_r(\delta_t) = \frac{1}{8} \cdot \lambda \cdot \rho \cdot a \cdot V_h(d, \delta(t))^3 \cdot \delta(t) \tag{13}$$

where λ represents a coefficient for the drag profile depending on the type of UAV considered. From Eq. (13), apart from λ, the bigger the rotor disks are (a) and the higher the horizontal speed is ($V_h(\delta_t)$), the greater impact on the UAV energy consumption. Therefore, the global energy consumption of an UAV during time period δ_t derived from MOV, and ASC/DESC actions is expressed in Eqs. (14), (15), respectively:

$$E^{\text{MOV}}(\delta_t) = E_h(\delta_t) + E_r(\delta_t) \tag{14}$$

$$E^{\text{ASC/DESC}}(\delta_t) = E_h(\delta_t) + E_v(\delta_t) + E_r(\delta_t) \tag{15}$$

To sum up, Table 2 summarizes the energy consumption model considered for UAVs depending on the action they are performing during time period δ_t.

3.5. UAVs/ground sites energy levels balance

This section describes the energy level balance of UAVs and ground sites after performing a specific action at a given TS t. The energy level of UAV d at TS t, l_d^t, is computed by applying Eq. (16):

$$l_d^t = \begin{cases} l_d^{t-1} & \text{if the UAV is staying at a site} \\ l_d^{t-1} + E^{\text{REC}} & \text{if the UAV is recharging} \\ l_d^{t-1} - E^{\text{COV}} & \text{if the UAV is covering} \\ l_d^{t-1} - E^{\text{MOV}} & \text{if the UAV is moving at same altitude} \\ l_d^{t-1} - E^{\text{ASC}} & \text{if the UAV is ascending} \\ l_d^{t-1} - E^{\text{DESC}} & \text{if the UAV is descending} \end{cases} \tag{16}$$

In general, the energy level of an UAV at current TS, t, is equal to the one in the previous TS, $t-1$, minus the energy consumption of

the action it is actually performing. In case the UAV is recharging, its energy level will be increased by E^{REC}, energy that is retrieved from the batteries attached to the SPs. Finally, if the UAV is just staying on a site, its energy level is not modified.

Similarly, the energy level b_s^t at TS t of a site s in which the SPs and batteries are installed is expressed by Eq. (17):

$$b_s^t = \begin{cases} b_s^{t-1} + E^{\mathrm{SP}} - E^{\mathrm{REC}} & \text{if an UAV is recharging} \\ b_s^{t-1} + E^{\mathrm{SP}} & \text{if no UAV is recharging} \end{cases} \tag{17}$$

The energy produced by the SPs at TS t, E^{SP}, is added to the current energy level of the site, b_s^{t-1}. In case of a recharging action by an UAV, the energy required for the charge, E^{REC}, is subtracted from the batteries of the site.

4. Problem formulation

The problem we aim to solve is formulated as a Mixed Integer Linear Programming (MILP). Let us denote with $\mathcal{Z}$ the set of areas in the scenario on which 5G coverage must be provided. Let us also denote with $\mathcal{S}$ the set of ground sites at which a set of SPs are installed. Thus, the set of places in the scenario is defined by $\mathcal{P} = \mathcal{Z} \cup \mathcal{S}$. A set $\mathcal{D}$ of UAVs is considered to cover all the areas in $\mathcal{Z}$ during a set $\mathcal{T}$ of TSs. The set $\mathcal{A}$ represents the set of actions that can be performed by an UAV at a particular TS, with $\mathcal{A} = \mathcal{A}^{\mathrm{ASC}} \cup \mathcal{A}^{\mathrm{DESC}} \cup \mathcal{A}^{\mathrm{MOV}} \cup \mathcal{A}^{\mathrm{COV}} \cup \mathcal{A}^{\mathrm{REC}} \cup \mathcal{A}^{\mathrm{STAY}}$, deriving the ascending/descending, moving, covering, recharging and staying actions, respectively. The energy consumption of performing action $a \in \mathcal{A}$ by UAV $d \in \mathcal{D}$ at TS $t \in \mathcal{T}$ is noted as $E_{d,a}^t$. This value is assessed according to the model defined in Section 3.4. In order to describe the MILP formulation, a set of decision variables must be previously defined:

- $f_{d,a}^t$ is a binary variable equal to 1 if UAV d is performing action a at TS t, 0 otherwise.
- c_z^t is a binary variable equal to 1 if area z is covered by an UAV at TS t; 0 otherwise.
- l_d^t is a continuous variable representing the energy level of UAV d at TS t.
- b_s^t is a continuous variable representing the battery level of ground site s at TS t.

Therefore, the optimal 3-D Energy-Efficient UAV Mission Planning (3DEE-UMP) problem is formulated as:

$$min \sum_{t\in\mathcal{T}} \sum_{d\in\mathcal{D}} \sum_{a\in\mathcal{A}} E_{d,a}^t \tag{18}$$

subject to

$$l_d^t \le l_d^{t-1} - \sum_{a\in\mathcal{A}^{\mathrm{ASC}}\cup\mathcal{A}^{\mathrm{DESC}}\cup\mathcal{A}^{\mathrm{MOV}}\cup\mathcal{A}^{\mathrm{COV}}} E_{d,a}^t + \sum_{a\in\mathcal{A}^{\mathrm{REC}}} E_{d,a}^t \qquad \forall d \in \mathcal{D}, t \in \mathcal{T} \tag{19}$$

$$b_s^t \le b_s^{t-1} + E_s^{\mathrm{SP}} \cdot N_s^{\mathrm{SP}} - \sum_{d\in\mathcal{D}} \sum_{a\in\mathcal{A}^{\mathrm{REC}}} E_{d,a}^t \qquad \forall s \in \mathcal{S}, t \in \mathcal{T} \tag{20}$$

$$\sum_{a\in\mathcal{A}} f_{d,a}^t = 1 \qquad \forall d \in \mathcal{D}, t \in \mathcal{T} \tag{21}$$

$$\sum_{d\in\mathcal{D}} \sum_{a\in\mathcal{A}^{\mathrm{COV}}} c_z^t = 1 \qquad \forall z \in \mathcal{Z}, t \in \mathcal{T} \tag{22}$$

$$L^{\mathrm{MIN}} \le l_d^t \le L^{\mathrm{MAX}} \qquad \forall d \in \mathcal{D}, t \in \mathcal{T} \tag{23}$$

$$B^{\mathrm{MIN}} \cdot N_s^B \le b_s^t \le B^{\mathrm{MAX}} \cdot N_s^B \qquad \forall s \in \mathcal{S}, t \in \mathcal{T} \tag{24}$$

The objective function of 3DEE-UMP is defined in Eq. (18), whose main goal is to minimize the global energy consumption of the UAV swarm throughout time. Term $E_{d,a}^t$ represents the energy consumption derived from action $a \in \mathcal{A}$, which is performed by UAV $d \in \mathcal{D}$ during TS $t \in \mathcal{T}$. If the full set of UAVs is considered, $\sum_{d\in\mathcal{D}}$, each of them performing a specific action, $\sum_{a\in\mathcal{A}}$, for each TS, $\sum_{t\in\mathcal{T}}$, the global energy consumption of the UAV swarm throughout time is obtained. Eq. (18) therefore minimizes this value, respecting the set of constraints defined through Eqs. (19)–(24).

Eq. (19) imposes the energy level constraint for each UAV d at each TS t according to Eq. (16) of Section 3.4, as the balance between the UAV energy level at TS $t-1$ minus the energy consumption of the current action in the set $\mathcal{A}^{\mathrm{ASC}} \cup \mathcal{A}^{\mathrm{DESC}} \cup \mathcal{A}^{\mathrm{MOV}} \cup \mathcal{A}^{\mathrm{COV}}$, plus the energy retrieved if the current action is recharging its batteries ($a \in \mathcal{A}^{\mathrm{REC}}$). Similarly, the energy level constraint for ground sites is imposed by Eq. (20), in which the energy level of each site s at each TS t is computed as the energy level at previous TS plus the energy produced by a SP at such site, E_s^{SP}, multiplied by the number of SPs, N_s^{SP}. If there are UAVs that are recharging their batteries at the site, the associated energy must be subtracted to the previous result. Eq. (21) preserves that each UAV d is performing exactly one action in the set $a \in \mathcal{A}$ at each TS t. In the same way, Eq. (22) guarantees that each area z is covered by exactly one UAV d at each TS t. Continuous variables l_d^t and b_s^t are constrained by minimum and maximum values in Eqs. (23)–(24), respectively. In particular, the energy level of UAVs d at TS t must be in the range $[L^{\mathrm{MIN}}, L^{\mathrm{MAX}}]$ (Eq. (23)). With the lower level L^{MIN}, 3DEE-UMP ensures that each UAV will be able to reach a site to recharge its batteries and complete a mission. Finally, the energy level of site s is enforced in the range $[B^{\mathrm{MIN}} \cdot N_s^B, B^{\mathrm{MAX}} \cdot N_s^B]$, where N_s^B is the number of batteries installed at site s (Eq. (24)).

5. GA for 3D energy-efficient UAVs mission planning

The problem formulation defined in Section 4, which generalizes the formulation for a multi-period capacitated network design problem, has been demonstrated in [26] to be NP-hard. In order to solve it in tractable time, in this section an efficient heuristic based on GAs is proposed. At first, the chromosome coding is provided. Then, the fitness function used to evaluate the suitability of each individual in the population is defined. Next, the description of the criteria used to create of the initial population as well as the genetic operators and functions applied throughout the set of generations are explained. Finally, a complexity analysis of the algorithm is provided.

5.1. Chromosome coding

In GAs, potential solutions to the problem are represented by chromosomes, structures composed of a set of genes which altogether define the nature of the individual. In our proposal, a chromosome c in the population $\mathcal{P}$ is defined by Eq. (25):

$$c = \{\underbrace{g_1^1, \ldots, g_{|\mathcal{D}|}^1}_{m_1}, \ldots, g_d^t, \ldots, \underbrace{g_1^{|\mathcal{T}|}, \ldots, g_{|\mathcal{D}|}^{|\mathcal{T}|}}\}_{\mathrm{m}_{|\mathcal{T}|}} \qquad \forall g_d^t \in c, d \in \mathcal{D}, t \in \mathcal{T} \tag{25}$$

where gene g_d^t refers to a specific UAV d in the swarm at TS t, $\forall d \in \mathcal{D}, t \in \mathcal{T}$. More formally, a gene is a 3-tuple of type $g_d^t = \{p_d^t, a_d^t, h_d^t\}$ in which p_d^t indicates the place id of UAV d after performing action a_d^t at altitude h_d^t during TS t. Table 3 depicts the admissible set of actions and their integer values for the chromosome coding.

Fig. 4 shows an example of chromosome codification for two consecutive TSs, t and $t+1$, which represents a potential solution for a scenario with 2 areas, $\mathcal{Z} = \{z_1, z_2\}$, 2 sites, $\mathcal{S} = \{s_1, s_2\}$, 2 altitudes, $\mathcal{H} = \{h_0, h_1\}$, and a swarm of 5 UAVs, $\mathcal{D} = \{d_1, d_2, d_3, d_4, d_5\}$. It can be seen that the two areas are covered by one UAV each during the two consecutive TSs. In particular, UAV d_2 is covering area z_1 at TS t. Then, in the next TS, d_4 replaces d_2 for covering the area, since this last descends toward site s_2 to recharge its batteries in the next TS. On the contrary, UAV d_1 remains covering area z_2 during the two TSs. With this toy case, all the actions defined in Table 3 are represented. With this codification, a chromosome $c \in \mathcal{P}$ represents a potential mission planning for the UAV

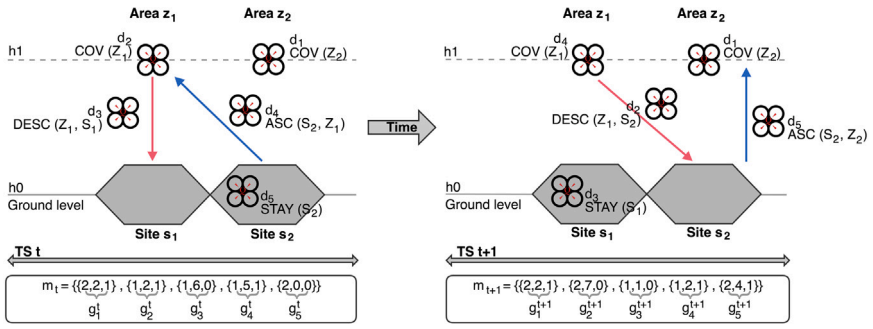

Fig. 4. Example of chromosome codification for two consecutive TSs in a scenario composed of 2 areas, 2 sites and 5 UAVs.

Table 3
Codification of action a_d^t for chromosome representation.

Code ID	Action	Altitude
0	STAY at site s_i	h_0
1	REC at site s_i	h_0
2	COV over area z_i	$h_k, k \in [1, \|\mathcal{H}\|]$
3	MOV from area z_i toward area z_j	$h_k, k \in [1, \|\mathcal{H}\|]$
4	ASC from place (site or area) p_i toward area z_i	$h_k, k \in [1, \|\mathcal{H}\|]$
5	ASC from place (site or area) p_i toward area z_j	$h_k, k \in [1, \|\mathcal{H}\|]$
6	DESC from area z_i toward place (site or area) p_i	$h_k, k \in [0, \|\mathcal{H}\| - 1]$
7	DESC from area z_i toward place (site or area) p_j	$h_k, k \in [0, \|\mathcal{H}\| - 1]$

swarm, D, during the whole set of TSs, $\mathcal{T}$. In order to become a solution to the problem, the mission planning derived from c must satisfy the constraints on UAVs energy level (Eqs. (19), (23)) and on the energy level of ground sites (Eqs. (20), (24)), as well as the coverage of all the areas in the scenario (Eq. (22)). If all the constraints are respected, c represents a solution and it must be evaluated according to a fitness function, which provides its suitability to the problem.

5.2. Fitness function

The fitness function defined to evaluate the goodness of a chromosome, $c \in \mathcal{P}$, is expressed in Eq. (26):

$$P(c) = \left(\sum_{g_d^t \in c} \omega(g_d^t) \right) \phi, \quad \forall d \in D, t \in \mathcal{T} \tag{26}$$

where function $\omega(g_d^t)$ returns the energy consumption associated to gene g_d^t, i.e., the one derived from the action carried out by UAV d at TS t according to the functions included in Table 2. Thus, the fitness function computes the aggregated energy consumption of the mission planning represented by the potential solution c for the UAV swarm during the whole set of TSs. The resulting value of the sum is multiplied by ϕ, which is set to 1 if the mission planning mapped by c is feasible, i.e., all the constraints defined in Eqs. (19)–(24) are respected. Otherwise, ϕ takes a value high enough to penalize the corresponding fitness value to such unfeasible chromosome.

5.3. Initial population and genetic operators

In order to obtain an energy-efficient mission planning, the individuals in the population must represent feasible missions which, through the application of successive generations, will converge to a (near) optimal mission in terms of energy consumption. For this reason, a set of $|\mathcal{P}|$ suitable missions are generated for the initial population of the GA. Rather than proposing a single scheme, several strategies are considered and combined to compose $\mathcal{P}$: (i) The first type of mission relies on a continuous coverage mode for UAVs during consecutive TSs, i.e., each UAV ascends from a site to an area in order to cover it during several TSs, up to reaching an energy level that forces it to descend to a site and recharge its batteries; (ii) The second type of mission is based on the principle described above, while also minimizing the required number of UAVs during the mission; (iii) The third type of mission is a generic mission starting from a site, ascending to an area, covering during ψ TSs and then returning to a site. We vary the value of ψ in order to provide a higher granularity to the initial population; (iv) Finally, random (but feasible) missions are generated by varying the number of UAVs placed on each site, the number of UAVs that must replace others in the next TS others, the number of consecutive covering actions per UAV, and the movement between areas.

Concerning the genetic operators that are used by 3DEE-UMP, the selection of individuals that survive and generate offspring follows the classical roulette wheel criterion, by applying single-point cross-over. With respect to the mutation of genes, a two-step process is followed: at first, every individual is divided into fractions that can be candidates for mutation. In such case, each gene is replaced by another valid value. These three functions (selection, cross-over and mutation) are executed in each generation before 3DEE-UMP halts after reaching the maximum number of allowed generations.

5.4. Complexity analysis

In the following, a complexity analysis is performed for 3DEE-UMP. Three aspects must be taken into account when assessing the complexity of a GA: (i) the length of chromosomes; (ii) the population size; and (iii) the complexity of the fitness function. In our proposed solution, each chromosome has a length of $|c| = |D| \cdot |\mathcal{T}|$ (Section 5.1). Furthermore, the fitness function defined in Section 5.2 takes $\mathcal{O}(|D| \cdot |\mathcal{T}|)$ for each chromosome in the population, and therefore $\mathcal{O}(|\mathcal{P}| \cdot |D| \cdot |\mathcal{T}|)$ for the entire population. While the selection function requires $\mathcal{O}(|\mathcal{P}|)$, crossover and mutation take $\mathcal{O}(|\mathcal{P}| \cdot |D| \cdot |\mathcal{T}|)$. Finally, the 3DEE-UMP resulting complexity is $\mathcal{O}(|\mathcal{P}| \cdot |D| \cdot |\mathcal{T}|)$.

6. Experimental results

In this section, a performance evaluation of the GA-based heuristic to solve the 3DEE-UMP problem is provided. At first, the description of the scenario over which the solution is applied is explained. Then, a set of performance analyses are carried out to evaluate the effectiveness of the proposed solution and to compare it with similar state-of-the-art approaches. Finally, a convergence and computational evaluation is provided.

6.1. Scenario description

We consider a rural scenario located in Plasencia (Spain), a town in the north of Extremadura with about 40,000 inhabitants mainly composed by small houses and lack of obstacles. Fig. 5(a) shows a map of the scenario in which the center of the areas to be covered are represented by blue pins. In order to define the number and location of ground sites, a minimum cost algorithm based on [27] has been

implemented to solve the network design problem. Result is shown in Fig. 5(b), where red circles represent the center of the areas and blue squares are the ground sites in which the SPs and batteries are installed, i.e., $|\mathcal{Z}| = 8$, $|S| = 3$. Thus, in the scenario, 3 places are areas and sites at the same time. The green circle represents the coverage area of an UAV that is covering z_2 at altitude h_1. The delimitation between places is assessed applying a Voronoi tessellation, for which the maximum distance between an UAV covering an area and its corresponding site with the HL BS functions (see Fig. 1) is enforced to be lower than a maximum value, μ. In the scenario, we set $\mu = 900$ [m] according to the application of the algorithm mentioned above [27]. This value has been experimentally obtained to guarantee the required QoS for the backhaul radio link established between the UAV and the site. By adopting this setting, the time to reach an area from a site (and vice-versa) is much lower compared to the TS duration.

If we now move our attention to the constraints affecting UAVs energy balance, L^{MIN} and L^{MAX} define the range of admissible values for UAVs battery level, which are set in accordance to [8]. With these values, we assume that each UAV has an amount of energy sufficiently high to safely land on a site upon an emergency and/or bad weather condition. Moreover, we also assume $E^{\text{REC}} = 1000$ [Wh], as in [8].

The power consumption of the BS radio to serve users is set to $P^{\text{BS}} = 200$ [W]. This value is chosen in accordance to a realistic setting [25]. The coefficient for the drag profile depends on the geometry of the rotor blades and is set to $\lambda = 0.08$ in accordance to [28]. Moreover, the maximum power of the motor is $P_s^{h_k} = 85$ [W], $\beta = 30$ [W], and $\alpha = 10.5$. They all depend on the UAV weight and the motor/propeller characteristics. In our simulations, we assume the values used in [24]. The optimal elevation angle, $\theta = 20.34°$, is set in accordance to [23]. Finally, the S-curve parameters, d, e, are set in accordance to Tabs. 1 and 2 of [23], as well as the carrier frequency: $f_c = 2000$ [MHz].

Concerning the features of the set of solar panels considered in the scenario, B^{MIN} and B^{MAX} are set in accordance to [29], with the aim of guaranteeing the recharge of UAVs, as well as to avoid possible battery failures. Finally, the number of solar panels and batteries in each site are obtained as output of the application of the solution defined in [27]. With respect to the energy production of SPs at ground sites, PVWatts calculator [30] has been used to exploit the realistic historical energy production of SPs in Plasencia obtained during the summer solstice (June 21st).

Finally, the type of considered UAV in the simulations is a quadcopter with DJI F-450 chassis of 750 watt rotors, 20,000 mAh LiPo battery and an Autopilot ArduPilot APM 2.6, which results in a weight of about 4 kg. Moreover, the average power consumption of this type of UAV results in 950 mAh with an electrical potential of 3.7 V. Thus, considering normal wind conditions (less than 5 Km/h) and pressure (1000 hPa), the battery can last approximately 37 min at a 25 km/h constant speed. Furthermore, specifications for the considered solar panels are 320 W of radiated power, 58.7 V of maximum power voltage and 6.46 A of maximum power current. Regarding the recharging actions performed by the UAVs, induction charging systems have been adopted as in [31], where automatic battery charge is performed through wireless power transfer technology. Table 4 summarizes the parameters and values used for the characterization of the considered scenario and simulations.

Table 4
Parameter setting for the considered scenario and simulations.

Parameter	Value/Reference	Parameter	Value/Reference
$\|\mathcal{Z}\|$	8	m	4 [kg] [9]
$\|S\|$	3	g	9.81 [m/s^2]
$\|\mathcal{H}\|$	2, 3	ρ	0.18 [m^2] [9]
$\|D\|$	20, 30, 40, 50	a	1.225 [kg/m^3] [9]
$\mathcal{T}$	1 day divided into TSs of $\delta_t = 10$ min	λ	0.08 [28]
P	20, 100, 200	d	See Tab. 1 of [23]
G	50, 100	e	See Tab. 2 of [23]
B^{MIN}	720 [Wh] [29]	f_c	2000 [MHz] [23]
B^{MAX}	2400 [Wh] [29]	θ	20.34° [23]
L^{MIN}	100 [Wh] [8]	β	30 [24]
L^{MAX}	1000 [Wh] [8]	α	10.5 [24]
P^{BS}	200 [W] [25]	$P_s^{h_k}$	85 [W] [24]
E^{REC}	1000 [Wh] [8]	μ	900 [m] [27]

6.2. Performance analysis

In the following, a set of performance analyses have been carried out to evaluate 3DEE-UMP over the considered scenario. They have been run on a dual-core Intel-based machine (@3.1 GHz) with 16 GB of RAM.

The first analysis aims at evaluating the outcomes of 3DEE-UMP when different altitudes can be used by the UAVs swarm. Our goal is to answer the next questions: (i) Which is the best setting in which the energy required by the mission planning is minimal and all the areas in the scenario are covered?; (ii) Is there any gain (in terms of energy efficiency or percentage of covered scenario) if the number of altitudes is larger than 2?; (iii) Which is the impact of adding UAVs to the swarm?

To shed light on these questions, different simulations have been run varying $|\mathcal{H}|$ and $|D|$. In case two altitudes are considered, $|\mathcal{H}| = 2$, with $h_0 = 0$ [m] (ground level) and $h_1 = 100$ [m] in accordance to a typical UAV setting [4], it has been experimentally checked that the minimum swarm size that is required for a successful mission planning throughout time is 17. Note that 8 UAVs must be always covering the set of areas, while additional ones can be performing the rest of actions. Based on this minimum number, we vary $|D| = \{20, 30, 40, 50\}$. If 3 altitudes are otherwise selected, $|\mathcal{H}| = 3$, the minimum number of UAVs increases up to 22, therefore the swarm size is set to $|D| = \{30, 40, 50\}$ for simulations with 3 altitudes. Regarding the TS duration, we select a TS of 10 minutes for a 24-hour time span. The considered TS duration is in line with the battery capabilities of currently available quadcopters UAVs [32]. In this way, we are able to control the UAV actions in a short time scale, while still allowing the solution of the problem instance to be obtained on a server machine. In order to better analyze the variations of results, we specifically focus on a subset of TSs, with $|\mathcal{T}| = 24$, which belong to the central hours of the day (from t_{61} to t_{84}) in which the SPs energy production is at its peak.

At first, we aim to show the insights of the results obtained by 3DEE-UMP simplest case, i.e., when two altitudes are considered ($|\mathcal{H}| = 2$) and the number of UAVs is small – yet feasible – to obtain a solution ($|D| = 20$). In this way, we can focus on type of missions that are performed by the UAVs (by looking the actions set of Fig. 6(a)), the variation in the battery level of each UAV (Fig. 6(b)) and their positioning over the territory (Fig. 6(c)).

Fig. 6(a) shows the actions performed by each UAV in each TS (figure best viewed in color). Remarkably, all of the UAVs are able to cover an area during 4 consecutive TSs. Then, they descend to an area (the same area or an adjacent one) in order to recharge their batteries in the next TS and ensure energy level constraints (Eq. (23)). Note that when the covering mission of an UAV is in its last TS, another UAV is moving to the same area in order to cover it in the next TS. Therefore, each area is continuously covered throughout time and no coverage interruptions are experienced.

In a similar way, the energy level l_d^t of each UAV in each TS is reported in Fig. 6(b). As expected, an UAV starts a mission with full battery, i.e., $L^{\text{MAX}} = 1000$ [Wh], and it is reduced while it is performing actions that consume energy (COV, ASC, DESC, MOV). In case the battery is approaching $E^{\text{MIN}} = 100$ [Wh], the UAV descends to a site in order to be recharged in the following TS. To give more insight, Fig. 6(c) reports the positioning of each UAV in each TS. Clearly, the positioning varies across time, e.g., an UAV can cover a specific area during its first mission, while it can move to another area in order to cover it during its second mission. Note that, although an UAV is covering the same area during 4 consecutive TSs (see, e.g., UAV 10

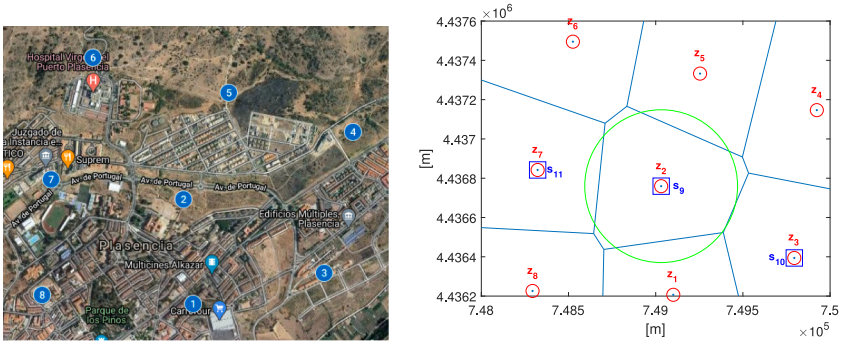

(a) Location of the places to be covered. (b) Location of the areas and sites.

Fig. 5. Plasencia scenario.

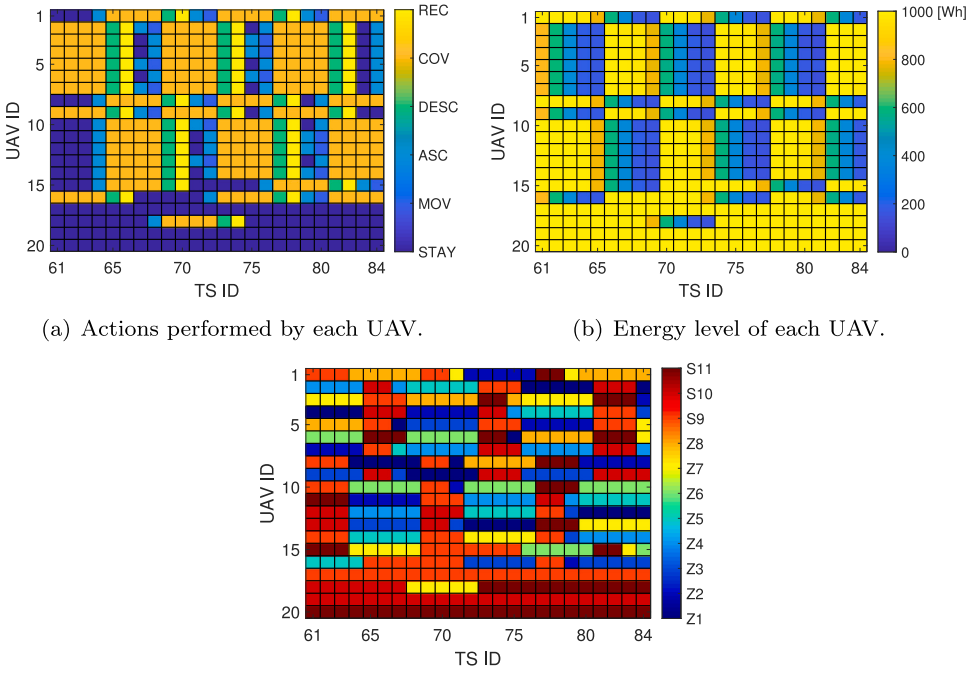

(a) Actions performed by each UAV. (b) Energy level of each UAV.

(c) Positioning of each UAV.

Fig. 6. Actions, energy level and positioning of each UAV for $|\mathcal{H}| = 2$, and $|D| = 20$.

during its first mission in Fig. 6(a) from TS t_{65} to t_{68}), in Fig. 6(c) it can be seen that it is placed at area z_6 during 5 consecutive TSs (starting at TS t_{64}). This is due to the fact that when the action involves a movement of type MOV, ASC, DESC, we select the UAV position as the destination place of such movement.

Once the results obtained by our solution for the case of 2 altitudes have been analyzed, we compare them with the results obtained by adding a new altitude, i.e., $|\mathcal{H}| = 3$ ($h_2 = 200$ [m]), and a bigger swarm of UAVs ($|D| = \{20, 30, 40, 50\}$). The objective of such analysis, which is reported in Figs. 7 and 8, is to check the benefits (if any) in terms of energy efficiency and/or percentage of covered scenario. The breakdown of cumulative actions considering different values of $|\mathcal{H}|$ and $|D|$ are reported in Fig. 7(a). By looking at the first group of bars, i.e., $C_1 = \{|\mathcal{H}| = 2, |D| = 20\}$, it can be seen that the type of action that is predominant is COV, which is a result of having 8 areas that must be covered during 24 TSs (192 actions). The next type of action that is more frequent for this configuration is STAY, mainly due to the subset of UAVs that do not perform any mission throughout the day (d_{17}, d_{19}, d_{20} in Fig. 6(a)). Actions requiring ascending from a site to an area or vice-versa (ASC, DESC) are equally balanced, taking an average of 45 actions for each of them, which is on the order of REC actions. Finally, the least frequent type of action is the movement between areas at same altitude (MOV), since the mission planning derived by the application of 3DEE-UMP tends to extend the covering phase instead of alternating covering and moving actions. If we now compare the results obtained for 2 and 3 altitudes with a swarm of 30 UAVs (C_2 vs. C_3), we can extract that the number of STAY actions is much higher for $|\mathcal{H}| = 2$, since there is a big number of unused UAVs compared to the case of $|\mathcal{H}| = 3$. Moreover, the number of ASC, DESC and MOV actions for a scenario in which there are 3 potential altitudes is higher compared to the one in which UAVs can be placed only at one altitude. Moreover, the distance to ground also results in larger ASC/DESC actions, with the corresponding energy consumption. This also results in more frequent REC actions. Finally, results obtained for C_4 follow a similar trend compared to C_3. However, a higher number of UAVs is associated with an increase of the energy consumption required by the mission planning, as well as a higher number of STAY actions.

In the following, we focus on the missions that are performed by the UAVs. Fig. 7(b) reports the obtained results considering minimum, average and maximum mission duration. Interestingly, when 2 altitudes are considered (left part of the figure), the average duration of UAVs missions is notably higher compared to the case of 3 altitudes (right

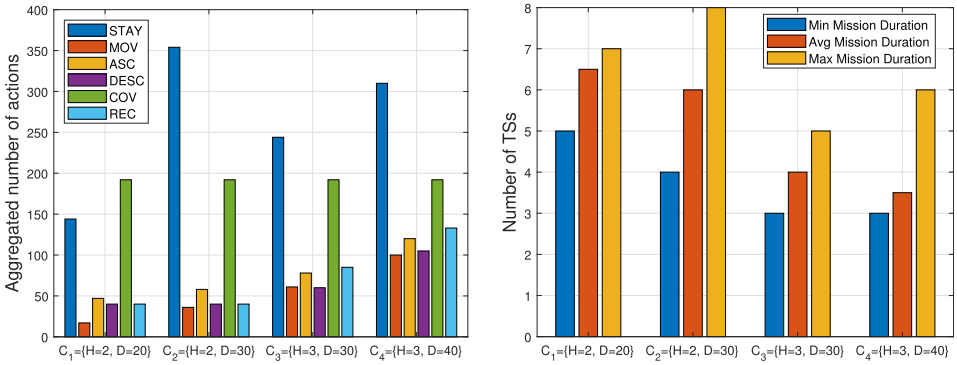

(a) Aggregated number of actions per type.

(b) Mission duration.

Fig. 7. Number of actions per type and duration of UAVs missions considering different altitudes and UAVs swarm size.

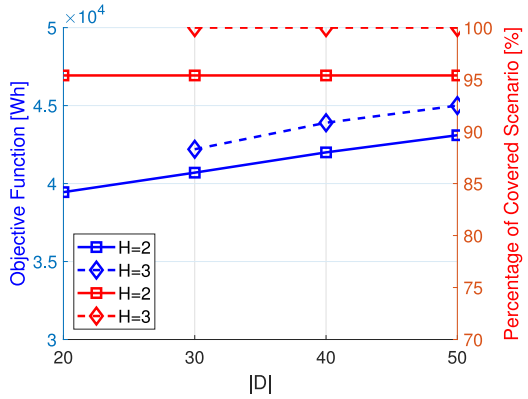

Fig. 8. Objective function (left axis) and percentage of covered scenario (right axis) as a function of the number of considered UAVs for $|H| = 2$ and $|H| = 3$.

part of the figure). For example, for C_2, the average duration of the UAV missions is 6 TSs, while they only last 4 TSs on average for C_3. This outcome is again a result of the energy that is required by UAVs that are covering at higher altitude and the distance they must travel when they are ascending to cover an area or descending toward the ground. Moreover, the number of UAVs in the swarm also impacts the mission duration: if the UAV swarm is bigger, more UAVs are prone to be used, which results in a general reduction in the average mission duration (compare C_1 with C_2, and C_3 with C_4). Finally, Fig. 8 reports in the left axis the values of the objective function defined in Eq. (26), which is produced as output by 3DEE-UMP for different values of $|D|$. By inspecting the figure, it can be seen that no point is reported for $|\mathcal{H}| = 3$ when the number of considered UAVs is $|D| = 20$. This is due to the fact that the minimum number of UAVs that are required for 3 altitudes in order to have a feasible solution is 22. Clearly, the objective function values increase with the UAV swarm size, both for 2 and 3 altitudes. Moreover, the best outcomes are obtained for $|\mathcal{H}| = 2$, with a difference about $0.17 \cdot 10^4$ [Wh] w.r.t. $|\mathcal{H}| = 3$. However, if we now focus on the percentage of covered scenario (right axis), the setting with 3 altitudes clearly outperforms the other one, reaching a percentage of covered scenario of 100%.

6.3. Comparison with other solutions

In order to compare the performance of our proposed solution with other approaches present in the state-of-the-art, two benchmark algorithms have been considered. The first solution is the one described in our previous work [8], namely Optimal Energy Management of UAV-based cellular networks (EMUC). In particular, the objective of this algorithm is the maximization of the energy stored by the set of UAVs and ground sites, while ensuring the coverage and energy constraints. The second benchmark algorithm is the one presented in [18], where the 3D coverage problem of UAVs is investigated. The goal of this algorithm, namely Log-linear learning based 3D UAV deployment (LL3D-UAV), is to maximize the coverage utility of the mission area with minimal transmission power by relying on a rotary-wing UAV group.

A performance analysis has been carried out to compare EMUC, LL3D-UAV and 3DEE-UMP over a 200 x 200 [m] scenario, which is described in [18]. The number of areas and sites required as input by EMUC and 3DEE-UMP, which result as output of the application of [27], is $|\mathcal{Z}| = 4$, $|\mathcal{S}| = 1$. The number of altitudes for LL3D-UAV and 3DEE-UMP has been set to $|\mathcal{H}| = 2$, since both works consider the 3D space. In case of EMUC, no altitude over the ground has been considered, i.e., $|\mathcal{H}| = 1$, with $h_0 = 0$ [m]. The number of TSs is 5, with a duration of 10 minutes each. For the rest of required parameters, we refer the reader to [8] for EMUC, [18] for LL3D-UAV, and this work for 3DEE-UMP.

Table 5 shows the breakdown of the obtained results. The first metric we consider is the aggregated energy consumption required by the solution to provide coverage over the target scenario. Remarkably, EMUC is the algorithm that presents the best results in terms of energy efficiency. Clearly, this is due to the fact that in such case the energy consumption derived by the 3D component (ascending/descending actions) is not considered, therefore leading to a reduction in the energy required by the solution. Among the two algorithms that take into account the altitude in their models, our solution slightly outperforms LL3D-UAV. It is in the percentage of covered scenario where the benefits achieved by 3DEE-UMP are more evident. While our solution guarantees coverage to almost the full territory (97.5%), a reduction in the total coverage utility is experienced by LL3D-UAV, reaching to 81.93% of the scenario. This situation is derived by the approximation followed by the algorithm, where the overall problem is decomposed into two subproblems. At first, the placement of the set of UAVs is performed in such a way that the coverage utility is maximized. Then, as a second step, the transmission power of UAVs is tuned to maximize the energy efficiency, which could lead to overlapping situations (see, e.g., Fig. 4 of [18]) in which a portion of the territory is not covered. The percentage of covered scenario is not reported for EMUC due to its 2D nature. Finally, both the average energy and battery levels of UAVs and sites are analyzed. With respect to these metrics, two considerations must be clarified. The first one is that no results are available for LL3D-UAV, since energy replenishment methods are not considered by the solution. The second aspect to remark is that EMUC outperforms 3DEE-UMP both in the average energy level per UAV as

Table 5
Performance evaluation of different solutions.

Metric	EMUC [8]	LL3D-UAV [18]	3DEE-UMP (This work)
Trajectory computation	2D ($\|\mathcal{H}\| = 1$)	3D ($\|\mathcal{H}\| = 2$)	3D ($\|\mathcal{H}\| = 2$)
Agg. energy consumption [Wh]	$6.91 \cdot 10^3$	$8.63 \cdot 10^3$	$8.47 \cdot 10^3$
Pct. of covered scenario [%]	*	81.93	97.5
Avg. energy level per UAV [Wh]	839.4	N/A	704.3
Avg. battery level per site [Wh]	$4.19 \cdot 10^3$	N/A	$3.15 \cdot 10^3$
Number of required UAVs	8	8	8

Table 6
Breakdown of the obtained results for $|D| = 30$.

Metric	$\|\mathcal{H}\|$	$P = 20$		$P = 100$		$P = 200$	
		$G = 50$	$G = 100$	$G = 50$	$G = 100$	$G = 50$	$G = 100$
Obj. function [Wh]	2	$4.32 \cdot 10^4$	$4.30 \cdot 10^4$	$4.25 \cdot 10^4$	$4.17 \cdot 10^4$	$4.12 \cdot 10^4$	$4.09 \cdot 10^4$
	3	$4.44 \cdot 10^4$	$4.42 \cdot 10^4$	$4.40 \cdot 10^4$	$4.34 \cdot 10^4$	$4.30 \cdot 10^4$	$4.24 \cdot 10^4$
Avg. energy level per UAV [Wh]	2	719.09	721.37	720.98	723.12	732.16	734.56
	3	534.65	540.32	541.73	545.54	550.04	557.18
Avg. battery level per site [Wh]	2	$3.35 \cdot 10^3$	$3.37 \cdot 10^3$	$3.38 \cdot 10^3$	$3.40 \cdot 10^3$	$3.41 \cdot 10^3$	$3.42 \cdot 10^3$
	3	$3.07 \cdot 10^3$	$3.09 \cdot 10^3$	$3.12 \cdot 10^3$	$3.15 \cdot 10^3$	$3.19 \cdot 10^3$	$3.23 \cdot 10^3$
Computation time [s]	2	1.27	2.28	1.98	2.53	2.26	3.12
	3	4.12	5.43	4.59	6.45	5.30	7.21
Number of required UAVs	2	17	17	17	18	18	20
	3	22	23	23	24	24	24
Pct. of covered scenario [%]	2	95.4	95.4	95.4	95.4	95.4	95.4
	3	98.7	99.6	100	100	100	100

well as in the average battery level per site. The reason is derived by the fact that the main goal of EMUC is to provide a 2D energy-efficient mission planning through the maximization of the energy stored by the UAVs and the one stored in the batteries of the ground sites, respecting coverage and energy constraints. In our work, instead, the main goal is to minimize the global energy consumption of the UAV swarm considering the 3D case, also satisfying the aforementioned constraints.

6.4. 3DEE-UMP convergence and computational evaluation

In the last part of our work, we aim to evaluate the performance of our proposed solution in terms of convergence and computational time. In general, the quality of the solution obtained by a GA improves with the number of generations during which it is being executed. Moreover, population size is another key parameter that must be evaluated. Table 6 shows the breakdown of the results obtained by 3DEE-UMP for $|D| = 30$, considering different values for the number of altitudes, $|\mathcal{H}|$, generations, G, and population size, P.

Several considerations emerge by inspecting Table 6. At first, the objective function values decrease with the size of the population, i.e., the larger the search space is, the better results obtained by 3DEE-UMP. The same consideration is extracted with respect to the number of generations. However, the gain of doubling the maximum number of generations before 3DEE-UMP halts is not as evident as in the case of the population size increase, especially if we consider the penalty imposed by the required computation time. As introduced in Section 5, the NP-hardness nature of the 3DEE-UMP problem defined in Section 4 requires a high amount of time to obtain the optimal solution, normally in the order of hours or even days. However, the proposed GA-based heuristic is able to retrieve a solution in few seconds at most, which means that it could be successfully re-run in real time if needed (e.g., due to sudden changes in the environment or potential failures). Therefore, our algorithm is a good candidate for the management of UAVs considering short time scales.

Results extracted from Fig. 8 are again confirmed in Table 6, where the possibility of considering 3 altitudes instead of 2 for the UAVs operation presents the drawback of requiring larger energy consumption for a suitable mission planning. However, if UAVs are able to cover at different altitudes ($|\mathcal{H}| = 3$), a larger percentage of the considered scenario is covered, reaching 100% for $P \geq 100$. This outcome is directly related with the minimum number of UAVs that are required by our algorithm to find a solution. Certainly, although a higher number is imposed by $|\mathcal{H}| = 3$, the difference w.r.t. $|\mathcal{H}| = 2$ is not excessive. Regarding the average energy level for UAVs and sites, it can be seen that the impact of the variation of parameters P and G is minimal when considering a specific value of $|\mathcal{H}|$. If we compare such results between $|\mathcal{H}| = 2$ and $|\mathcal{H}| = 3$, the larger energy consumption of UAVs covering at higher altitudes clearly impacts their energy level throughout time, as well as the duration of their missions, forcing them to recharge more frequently at ground sites. Thus, the average battery level at sites is also lower compared to $|H| = 2$.

7. Conclusion and future work

Although the percentage of people living outside of areas covered by mobile broadband networks has been reduced from 24% to 10% of the global population in the recent years, the coverage gap in rural and low-income areas still remains around 40%. The lack of access to the Internet by communities living in these locations impacts their welfare in terms of reduction of opportunities. In order to be part of the solution to this problem, this work proposes a theoretical model whose goal is to efficiently schedule the set of missions of a swarm of UAVs in order to provide cellular coverage over this type of scenarios, with minimal energy consumption. In particular, the formalization of the problem of providing coverage to rural areas while minimizing the energy consumption of the swarm of UAVs that are able to operate at different altitudes (3DEE-UMP) is provided. In order to practically solve the problem, a GA-based heuristic is defined and evaluated over a realistic scenario. Results indicate that a higher granularity in the number of altitudes at which UAVs can provide coverage increases the percentage of territory that is covered, while a small penalty on the energy consumption must be paid w.r.t. the case in which only one altitude over the ground is considered. As future steps, a study on the QoS perceived by users depending on the altitude at which UAVs are covering and the interference among UAVs covering adjacent areas can be carried out. The investigation of the optimal TS duration given a specific UAV model and the target scenario is also an interesting topic. Moreover, the benefits of adding other renewable energy sources in the architecture can also be evaluated.

Declaration of competing interest

The authors declare that they have no known competing financial interests or personal relationships that could have appeared to influence the work reported in this paper.

Acknowledgments

This work has been partially funded by the project RTI2018-094591-B-I00 (MCI/AEI/FEDER,UE), the 4IE+ Project (0499-4IE-PLUS-4-E) funded by the Interreg V-A España-Portugal (POCTEP) 2014–2020 program, and by the Department of Economy, Science and Digital Agenda of the Government of Extremadura (GR18112, IB18030).

References

[1] K. Bahia, S. Suardi, The State of Mobile Internet Connectivity 2019, Tech. Rep., GSMA Connected Society, 2019.
[2] C. Handforth, Closing the Coverage Gap. How Innovation Can Drive Rural Connectivity, Tech. Rep., GSMA Connected Society, 2019.
[3] A. Fotouhi, H. Qiang, M. Ding, M. Hassan, L.G. Giordano, A. Garcia-Rodriguez, J. Yuan, Survey on UAV cellular communications: Practical aspects, standardization advancements, regulation, and security challenges, IEEE Commun. Surv. Tutor. 21 (4) (2019) 3417–3442.
[4] M. Mozaffari, W. Saad, M. Bennis, Y. Nam, M. Debbah, A tutorial on UAVs for wireless networks: Applications, challenges, and open problems, IEEE Commun. Surv. Tutor. 21 (3) (2019) 2334–2360.
[5] Altaeros, 2021, Available: http://www.altaeros.com/. Accessed: 2021-02-19.
[6] Loon project, 2021, Available: https://loon.com/. Accessed: 2021-02-19.
[7] O. Magnussen, G. Hovland, M. Ottestad, Multicopter UAV design optimization, in: IEEE/ASME 10th International Conference on Mechatronic and Embedded Systems and Applications (MESA), 2014, pp. 1–6.
[8] L. Amorosi, L. Chiaraviglio, J. Galán-Jiménez, Optimal energy management of UAV-based cellular networks powered by solar panels and batteries: Formulation and solutions, IEEE Access 7 (2019) 53698–53717.
[9] Y. Sun, D. Xu, D.W.K. Ng, L. Dai, R. Schober, Optimal 3D-trajectory design and resource allocation for solar-powered UAV communication systems, IEEE Trans. Commun. 67 (6) (2019) 4281–4298.
[10] N. Babu, K. Ntougias, C.B. Papadias, P. Popovski, Energy efficient altitude optimization of an aerial access point, in: 2020 IEEE 31st Annual International Symposium on Personal, Indoor and Mobile Radio Communications, 2020, pp. 1–7.
[11] X. Lin, R. Wiren, S. Euler, A. Sadam, H.-L. Maattanen, S. Muruganathan, S. Gao, Y.-P.E. Wang, J. Kauppi, Z. Zou, et al., Mobile network-connected drones: Field trials, simulations, and design insights, IEEE Veh. Technol. Mag. 14 (3) (2019) 115–125.
[12] Y. Xu, L. Xiao, D. Yang, Q. Wu, L. Cuthbert, Throughput maximization in multi-UAV enabled communication systems with difference consideration, IEEE Access 6 (2018) 55291–55301.
[13] Y. Zeng, Q. Wu, R. Zhang, Accessing from the sky: A tutorial on UAV communications for 5G and beyond, Proc. IEEE 107 (12) (2019) 2327–2375.
[14] M. Alzenad, A. El-Keyi, F. Lagum, H. Yanikomeroglu, 3-d placement of an unmanned aerial vehicle base station (UAV-BS) for energy-efficient maximal coverage, IEEE Wirel. Commun. Lett. 6 (4) (2017) 434–437.
[15] B. Perabathini, K. Tummuri, A. Agrawal, V.S. Varma, Efficient 3D placement of UAVs with QoS assurance in ad hoc wireless networks, in: 2019 28th International Conference on Computer Communication and Networks (ICCCN), IEEE, 2019, pp. 1–6.
[16] Z. Yuan, J. Jin, L. Sun, K.-W. Chin, G.-M. Muntean, Ultra-reliable IoT communications with UAVs: A swarm use case, IEEE Commun. Mag. 56 (12) (2018) 90–96.
[17] H. Shakhatreh, A. Khreishah, J. Chakareski, H.B. Salameh, I. Khalil, On the continuous coverage problem for a swarm of UAVs, in: 2016 IEEE 37th Sarnoff Symposium, IEEE, 2016, pp. 130–135.
[18] X. Yu, J. Yao, L. Ruan, K. Yao, D. Liu, R. Chen, 3D deployment of multi-UAV for energy-saving: A game-based learning approach, in: 2019 IEEE 5th International Conference on Computer and Communications (ICCC), IEEE, 2019, pp. 1332–1337.
[19] Z. Kang, C. You, R. Zhang, 3D placement for multi-UAV relaying: An iterative gibbs-sampling and block coordinate descent optimization approach, IEEE Trans. Commun. (2020).
[20] J. Lu, S. Wan, X. Chen, P. Fan, Energy-efficient 3D UAV-BS placement versus mobile users' density and circuit power, in: 2017 IEEE Globecom Workshops (GC Wkshps), IEEE, 2017, pp. 1–6.
[21] S. Shakoor, Z. Kaleem, D.-T. Do, O.A. Dobre, A. Jamalipour, Joint optimization of UAV 3D placement and path loss factor for energy efficient maximal coverage, IEEE Internet Things J. (2020).
[22] S. Ortiz, C.T. Calafate, J.-C. Cano, P. Manzoni, C.K. Toh, A UAV-based content delivery architecture for rural areas and future smart cities, IEEE Internet Comput. 23 (1) (2018) 29–36.
[23] A. Al-Hourani, S. Kandeepan, S. Lardner, Optimal LAP altitude for maximum coverage, IEEE Wirel. Commun. Lett. 3 (6) (2014) 569–572.
[24] D. Zorbas, L. Di Puglia Pugliese, T. Razafindralambo, F. Guerriero, Optimal drone placement and cost-efficient target coverage, J. Netw. Comput. Appl. 75 (2016) 16–31.
[25] B.H. Jung, H. Leem, D.K. Sung, Modeling of power consumption for macro-, micro-, and RRH-based base station architectures, in: 2014 IEEE 79th Vehicular Technology Conference (VTC Spring), 2014, pp. 1–5.
[26] F. D'Andreagiovanni, J. Krolikowski, J. Pulaj, A fast hybrid primal heuristic for multiband robust capacitated network design with multiple time periods, Appl. Soft Comput. 26 (2015) 497–507.
[27] L. Chiaraviglio, L. Amorosi, N. Blefari-Melazzi, P. Dell'Olmo, C. Natalino, P. Monti, Optimal design of 5g networks in rural zones with UAVs, optical rings, solar panels and batteries, in: 2018 20th International Conference on Transparent Optical Networks (ICTON), 2018, pp. 1–4.
[28] J.M. Seddon, S. Newman, Basic Helicopter Aerodynamics, third ed., Wiley, Hoboken, NJ, USA, 2011.
[29] Y. Zhang, M. Meo, R. Gerboni, M. Ajmone Marsan, Minimum cost solar power systems for LTE macro base stations, Comput. Netw. 112 (2017) 12–23.
[30] PVWatts calculator, 2021, Available: https://pvwatts.nrel.gov/. Accessed: 2021-02-19.
[31] C. Song, H. Kim, D.H. Jung, K. Yoon, Y. Cho, S. Kong, Y. Kwack, J. Kim, Three-phase magnetic field design for low EMI and EMF automated resonant wireless power transfer charger for UAV, in: 2015 IEEE Wireless Power Transfer Conference, WPTC 2015, Institute of Electrical and Electronics Engineers Inc., 2015.
[32] Impossible aerospace US-1 performance aircraft, 2021, Available: https://secureservercdn.net/198.71.233.129/m3y.31e.myftpupload.com/wp-content/uploads/2020/06/Printer-Friendly-US-1-Data-Sheet-VS2.pdf. Accessed: 2021-02-19.

Jaime Galán-Jiménez received his Ph.D. in Computer Science and Communications from the University of Extremadura (Spain) in 2014. He is currently working at the Computer Science and Communications Engineering Department, University of Extremadura, as an assistant professor. During the past years, he has spent several research and teaching periods at University of Rome Tor Vergata, and at University of Rome La Sapienza, Italy. His main research interests are Software-Defined Networks, UAV-based 5G networks planning and design, 5G provisioning in rural and low-income areas and Mobile Ad-Hoc Networks.

Enrique Moguel works as a Researcher at the University of Extremadura (Spain). He received a MSc. in Computer Science at the University Carlos III (Spain) in 2010, and a Ph.D. in Computer Science at the University of Extremadura in 2018. His research interests include Web Engineering, Smart Cities and Ambient Intelligence. He has more than 25 relevant publications in journals and conferences related to these areas.

Jose Garcia-Alonso is an associate professor in the Department of Computer and Telematics Systems Engineering at the University of Extremadura (Spain) and co-founder of the Startups Gloin and Viable. He received a Ph.D. degree (with European Mention) in 2014. His main research interests are eHealthCare, eldercare, Mobile Computing, Context-Awareness and Pervasive Systems. He has published more than 80 research works in different international journals and conferences. As the PI of several projects he has managed more than €1M in research funds and organized several international scientific activities.

Javier Berrocal is an associate professor in the Department of Computer and Telematic Systems Engineering at the University of Extremadura (Spain). He received the Ph.D. degree in computer science from the University of Extremadura, Spain, in 2014. His main research interests are software architectures, mobile computing, Cloud-IoT computing, context-awareness, user profiling. He has published more than 100 academic papers in peer-reviewed conferences and journals, and has served as a reviewer for several journals, conferences and workshops.